Astron. Astrophys. 363, 605–616 (2000)

ASTRONOMY AND ASTROPHYSICS

Lithium and mass loss in massive AGB stars in the Large Magellanic Cloud

P. Ventura[1], **F. D'Antona**[1], **and I. Mazzitelli**[2]

[1] Osservatorio Astronomico di Roma, 00040 Monte Porzio Catone (Rome), Italy (paolo@coma.mporzio.astro.it)
[2] Istituto di Astrofisica Spaziale C.N.R., Via Fosso del Cavaliere, 00133 Rome, Italy (aton@hyperion.ias.rm.cnr.it)

Received 21 April 2000 / Accepted 5 September 2000

Abstract. The aim of this work is to use full evolutionary models to derive observational constraints on the mass loss rate of the upper Asymptotic Giant Branch (AGB) stars. The observations used to constrain the models are: i) the relative number of luminous Lithium rich AGBs in the Magellanic Clouds, with respect to the total number of AGBs populating the luminosity range $-6 \geq M_{\rm bol} \geq -7$; ii) the s-process enhancement of the same sample. The calibration of the mass loss rate we obtain gives feedbacks on the interpretation of observational data of obscured AGBs, and allows us to provide consistent lithium yields for these stars, to be used to constrain the galactic chemical evolution.

We find that: a) we can put lower and upper limits to the mass loss rate during the AGB phase; b) after a "visible" phase, the models evolve into a phase of strong mass loss, which can be identified with the obscured OH/IR stars accessible only in the infrared; the models well reproduce the Period-$M_{\rm bol}$ loci of the obscured AGBs (Wood et al. 1992); c) the most massive AGBs (mass of progenitors, hereinafter M_{ZAMS}, $\sim 6M_{\odot}$) are extremely luminous ($M_{\rm bol} \sim -7.2$ to -7.5); d) The lithium yield increases with the mass loss rate and with the total stellar mass, being maximum for AGB stars close to the lower limit for carbon semi-degenerate ignition. However, the mass loss calibration obtained in this work implies that massive AGBs *do not* contribute significantly to the lithium enrichment of the interstellar medium.

Key words: stars: AGB and post-AGB – stars: evolution – stars: mass-loss

1. Introduction

Following the pioniering studies by Schwarzschild & Harm (1965, 1967) and Weigert (1966), it is now a quarter century since the first extensive modeling of Asymptotic Giant Branch (AGB) structures, in which, above the carbon oxygen core, hydrogen and helium alternatively burn in shells, with the He-burning phase being initiated by a thermonuclear runaway (Thermal Pulse – TP – phase, e.g. Iben 1981). The convective shells developped during the TPs, and the following "dredge up" of inner nuclearly processed material to the surface (Iben 1975) leads to the formation of Carbon and s-process enhanced stars. Already two decades ago (see Iben 1981) it was realized that in the LMC, where the AGB luminosities are more reliable than in the Galaxy, there were no Carbon stars more luminous than $M_{\rm bol} \sim -6$ (Blanco et al. 1980), contrary to the theoretical expectations on the extension of the AGB up to $M_{\rm bol} \gtrsim -7$. This old finding is confirmed by recent studies (Costa & Frogel 1996).

Later on, very luminous AGBs were discovered (Wood et al. 1983): they were oxygen rich (M-type) stars, and were few compared to the numbers expected if massive AGBs evolve at the theoretical nuclear rate of $\sim 1{\rm mag}/10^6{\rm yr}$. This is confirmed also by the scarciness of these stars in the MCs clusters (e.g. Frogel et al. 1980, Mould & Reid 1987).

It is generally accepted that the lack of a C-star stage above $M_{\rm bol} \sim -6$ is due to nuclear processing at the bottom of the convective mantle of massive AGBs (Hot Bottom Burning, HBB), which cycles into nitrogen the carbon dredged up, if any (Iben & Renzini 1983, Wood et al. 1983). This interpretation has been widely confirmed by the discovery that *almost all* the luminous oxygen rich AGBs in the MCs are lithium rich, that is they show at the surface a lithium abundance $\log(\epsilon(^7Li)) > 2$ (where $\log(\epsilon(^7Li)) = \log(^7Li/H) + 12$) (Smith & Lambert 1989, 1990; Plez et al. 1993; Smith et al. 1995; Abia et al. 1991). Production of lithium is possible via the so-called Cameron & Fowler (1971) mechanism, if the temperature at the bottom of the convective envelope is $T_{\rm bce} \gtrsim 4 \times 10^7$K and non instantaneous mixing is accounted for. Modelling of HBB started early with envelope models including non instantaneous mixing coupled to the nuclear evolution (Sackmann et al. 1974) and the lithium production is well reproduced in the recent full models (Sackmann & Boothroyd 1992; Mazzitelli et al. 1999 – hereinafter MDV99 –; Blöcker et al. 2000). Although the details of lithium production depend on the input physics, mainly on the modelling of convection (MDV99), the luminosity range at which lithium rich AGBs should appear is not sensibly dependent on the details, and agrees well with the range observed in the MCs, namely $-6 \gtrsim M_{\rm bol} \gtrsim -7$. Let us recall that modelization of the lithium production in AGB is necessary to understand the galactic chemical evolution of lithium from the population II values $\log(\epsilon(^7Li)) \sim 2$ (Spite & Spite 1993; Boni-

Send offprint requests to: P. Ventura

facio & Molaro 1997) to the present solar system abundance of $\log(\epsilon(^7Li)) \sim 3.3$ (see Romano et al. 1999 for a recent reevaluation of the problem).

The scarciness of luminous AGBs, on the other hand, must be attributed to the onset of strong mass loss which terminates the "visible" evolution and leads to a phase in which the stars are heavily obscured by a circumstellar envelope (CSE) and eventually evolve to the white dwarf stage. This occurs when matter of the outermost layers is found at a distance from the star where temperature and density allow for dust formation, and collisional coupling of the grains with the gas drives a very efficient stellar wind (Habing et al. 1994; Ivezic & Elitzur 1995). The stars will then traverse a phase during which they are surrounded by a thick CSE.

A major problem in building up realistic upper AGB models is then the modelization of mass loss, a necessary ingredient from several independent points of view. For the nucleosynthesis and galactic chemical evolution, the yields from massive AGBs (in particular the lithium yields, as we will see in the present calculations) are influenced by mass loss during the HBB phase, not only because different amounts of processed envelopes are shed to the interstellar medium at a given time (reflecting the stage of nucleosynthesis which has been reached), but also because the stellar structure, and thus $T_{\rm bce}$ and the nucleosynthesis itself, depends on the rate of mass loss: therefore selfconsistent models must be explored and they have not yet been developped.

On the other hand, while at first the searches for AGB stars in the Galaxy and the MCs had been limited to optically bright stars, the surveys in the infrared, starting from IRAS databases or from near IR observations, are making the cornerstones for the understanding of the phase during which, by heavy mass loss, the objects become enshrouded in dust, making them practically invisible at the optical wavelengths and accessible only in the infrared (e.g. Habing 1996). Based on these surveys (see, e.g., Zijlstra et al. 1996; van Loon et al. 1997), follow up observations have given information on the pulsation periods; mass loss rates ($\dot{M}$) and expansion velocity of the envelope have been derived via the OH/IR associated masers (e.g. Wood et al. 1992); ISO spectroscopy and/or photometry has allowed to model the bolometric luminosity and $\dot{M}$ (e.g. van Loon et al. 1999a). The obscured AGBs observations will be a powerful test for the stellar models expected to have extended CSE. [1]

In MDV99 we presented results from detailed computations focused on lithium production in massive AGB stars, with the aim of studying the influence of convection modelling and other physical inputs on the surface lithium abundance. Although the models were run for population I composition stars, a first comparison with the LMC and SMC lithium rich AGBs was attempted (Fig. 16 in MDV99). However, a full and more detailed comparison with the MCs requires models computed with the appropriate metallicity. Further, in MDV99 we did not touch the problem of visibility and of a possible calibration of mass loss.

In this paper we present stellar models starting from the pre-main sequence and evolved to the AGB phase, with different prescriptions for $\dot{M}$, with the aim to describe the lithium rich AGBs observed in different luminosity bins in the MCs bright sources. A further constraint can be put based on the s-process enrichment observed in these same stars.

We compare the paths of evolutions having $\dot{M}$ consistent with these observations with the $\dot{M}$ versus pulsation period observations of obscured stars in the LMC (Wood et al. 1992) and with the $\dot{M}$ versus $M_{\rm bol}$ derived from ISO spectrophotometry (van Loon et al 1999a).

We finally show how the models vary with the main physical inputs. In particular we find that, within the framework of our convection model, the lithium vs. luminosity trend is not influenced by the overshooting distance, but this latter is relevant to determine the range of masses involved in lithium production, which our computations show to be extablished within $0.5M_{\odot}$. The minimum mass achieving HBB leading to large lithium abundances is slightly dependent on the mass loss rate adopted, lowest $\dot{M}$ models having more chances of achieving high temperatures at the base of the external envelope during their AGB evolution.

These new tracks represent a first numerical attempt to quantify the mass loss in the massive AGB evolution. The mass loss parametrization has a number of implications on the problems of population synthesis and galactic chemical evolution, whose modeling remains very qualitative if it is not based on such full computations. In particular, the calibration we obtain implies that the lithium production from the massive AGB stars is not relevant for the lithium galactic chemical evolution.

2. Macro physics input

The numerical structure of the ATON2.0 code, as well as a complete description of the physical inputs, can be found in Ventura et al. (1998). The description of the modeling of lithium production is in MDV99. We remind here the main formulations and describe the new inputs introduced especially for this work.

2.1. Diffusive scheme and overshooting

Mixing of chemicals and nuclear burning are self-consistently coupled by solving for each of the elements included in the nuclear network the diffusive equation:

$$\frac{dX_i}{dt} = \left(\frac{\partial X_i}{\partial t}\right)_{\rm nucl} + \frac{\partial}{\partial m}\left[(4\pi r^2\rho)^2 D \frac{\partial X_i}{\partial m}\right]$$

being X_i the chemical abundance of the i-th element and D the diffusive coefficient.

In the context of diffusive mixing also the formulation of overshooting assumes a meaning more physically sound: we do not simply assume an extra-mixing down to a fixed distance away from the formal convective border (established according

[1] Actually, the carbon stars at $M_{\rm bol} < -6$ found among *obscured* AGBs in the MCs (van Loon et al. 1999b) do not change the interpretation of the above scenario: this sample can represent the latest phases of AGB evolution (Frost et al. 1998), during which the strong mass loss cools the convective envelope and the dredged-up carbon is no longer cycled.

to the Schwarzschild criterium), but we allow an exponential decay of velocity outside convective regions of the form

$$v = v_b exp \pm \left(\frac{1}{\zeta f_{\rm thick}} ln \frac{P}{P_b} \right)$$

The exponential decay is consistent (at least on a qualitative ground) with approximate solutions of the Navier-Stokes equations (Xiong 1985; Grossman 1996), and with the results of numerical simulations (Freytag et al. 1996). In the above expression v_b and P_b are the values of convective velocity and pressure at the convective border, $f_{\rm thick}$ is the width of the whole convective region in fractions of H_p, and ζ is a free parameter giving the e-folding distance of the exponential decay, which we already tuned by comparing with the width of the main sequence of some open clusters: a conservative estimate indicates that a value $\zeta = 0.02$ is required (Ventura et al. 1998). A value of $\zeta = 0.03$ may be required from consideration of other evolutionary phases (Ventura et al. 2000, in preparation).

2.2. Symmetric overshooting

The necessity of the existence of some overshooting away from convective borders was strengtened by the difficulty of fitting the width of the main sequences of popI open clusters without allowing any extra mixing from the Schwarzschild border (Maeder & Meynet 1989; Stothers & Chin 1991): for these hystorical reasons the term "overshooting" has been associated to extra mixing from the convective core during the phases of central burning (Meynet et al. 1993), while few models exist which take into account also overshooting from the base of the convective envelope (Alongi et al. 1991). For AGBs, the luminosity evolution of models with low core masses and overshooting below the border of the outermost convective zone, and the possible implications for the efficiency of the third dredge-up and the core mass - luminosity relationship is explored by Herwig et al. (1997). The influence of symmetric overshooting on the evolution of the most massive AGBs close to the limit of carbon ignition is discussed in MDV99. Further, Ventura et al. (1999) show the possibility of reproducing the evolution of lithium rich C-stars with a small amount of overshooting "from below" the base of the external envelope. Here we do not address the issue of the extension of such extra-mixing region, nor the changes of the surface abundances of the elements other than lithium introduced by such extra-mixing: we simply focus our attention on the influence of overshooting "from below" on the lithium vs. luminosity trend in Sect. 5.1

It is therefore clear that at present we cannot give a full description of the s-process enhancement, which is the outcome of dredge-up mixing material from the He-burning shell to the surface following each TP. Yet, it appears evident that this enhancement can be detected only after some TPs have taken place, and this will be a strong constrain to choose the appropriate mass loss rate, if we consider that the luminous Li-rich AGBs in the MCs are all s-process enhanced.

In the following, we refer to models without overshooting below the base of the envelope as "standard".

2.3. Convection

Our code can use two local models for the evaluation of the convective flux: the mixing lenght theory (MLT) and the Full Spectrum of Turbulence (FST) model (Canuto & Mazzitelli 1991, 1992). We remember that the FST model is more physically sound, since the whole spectrum of eddies is taken into account to obtain the convective flux, and the fluxes are consistent with experimental values (Lesieur 1987). In addition, MDV99 showed that for the issue of lithium production the FST gives results independent of the tuning of the model, at variance with the MLT case, where a much larger freedom of results can be obtained by tuning the mixing lenght parameter (Sackmann & Boothroyd 1992). In this work we use the FST model in its recent version, which employs the fluxes from Canuto et al. (1996).

2.4. Pulsation periods

To be able to compare our theoretical tracks with the stars of the above surveys we computed periods of our models by assuming that variable AGB stars are pulsating in the fondamental mode, according to Vassiliadis & Wood (1993):

$$\log(P) = -2.07 + 1.94 \log(R) - 0.9 \log(M)$$

where the period P is given in days, and the stellar radius R and mass M are expressed in solar units.

2.5. Mass loss

As we have shortly seen in the introduction, mass loss has to be taken into account in AGB computations, since AGBs may lose mass at such huge rates ($\dot{M} > 10^{-5} M_\odot$ yr^{-1}) (van Loon et al. 1999a) that the general path of their evolution can be substantially altered. As no "first principle" approach to mass loss exists, the compromise is to try to adopt a description based on a sound physical approach, although it needs calibration. Our choice for the present study relies on Blöcker's (1995) formulation, which is based on Bowen's (1988) detailed numerical hydrodynamic and thermodynamic calculations carried out for the dynamic atmospheres of models for long period variables evolving along the AGB both in solar and smaller than solar metallicities (Willson et al. 1996). Computation of extensive grids of models showed the extreme sensitivity of the mass loss rate to the stellar parameters: $\dot{M}$ becomes strongly dependent on luminosity during the AGB evolution. Blöcker (1995) starts from the usual Reimer's formulation. This is completely inadequate to describe the fast increase of the mass loss rate during AGB, (e.g. Habing 1996), so he introduces a further dependence on a power of the luminosity. The complete expression is:

$$\dot{M} = 4.83 \cdot 10^{-9} M^{-2.1} L^{2.7} \dot{M}_R$$

where $\dot{M}_R$ is the canonical Reimers rate expressed by

$$\dot{M}_R = 4 \cdot 10^{-13} \eta_R \frac{LR}{M}$$

Tuning of the parameter η_R is one of the goals of the present work.

The dependence of the mass loss rate on the stellar parameters is far from being settled in Blöcker formulation: it is useful to compare our main results with other suggestions for $\dot{M}$ recently appeared in the literature. Salasnich et al. (1999) provide a prescription for $\dot{M}$ which has as a basis an empirical relationship between $\dot{M}$ and pulsation period (Feast 1991), including also the effects of a systematic variation of the dust to gas ratio at increasing luminosities:

$$\log(\dot{M}) = 2.1 \cdot \log(L/L_{\odot}) - 14.5$$

The above relation depends on the luminosity only, and, if reliable, it would make less critical the uncertainties connected with, e.g., the convective model adopted, from which the $T_{\rm eff}$ of the star depends strongly (D'Antona & Mazzitelli 1996, MDV99)

A strong dependence on the effective temperature ($\sim T_{\rm eff}^{-8}$) has been suggested (Schroeder at al. 1998) to trigger a large increase of $\dot{M}$ at low temperatures with respect to the Blöcker's recipe. Although this formulation has been developped for Carbon stars, we will test it to show how the strong dependence on $T_{\rm eff}$ counterbalances the effect of the decreasing luminosity on $\dot{M}$ in the latest stages of evolution.

Remember however that these formulas are still to be considered strictly a parametric exploratory approach.

2.6. Model observability

The models we build up provide as observables the bolometric luminosity, the photospheric $T_{\rm eff}$ (obtained through a grey atmosphere integration) and $\dot{M}$. If we wish to compare the results to selected samples of stars, we need to compute bolometric corrections and colors and, when $\dot{M}$ becomes important, we have to worry about the presence of an optically thick CSE, and should compute how the photospheric quantities are modified by the envelope. Although this kind of approach is in preparation (Groenewegen & Ventura 2000 in preparation), for the present work we mainly need to understand whether the models we build up correspond to stars which emit a good fraction of light into near IR wavelengths (so that they could be easily discovered in the K band surveys) and whether the optical red part of the spectrum – including the lithium line – is observable. When the mass loss becomes too large, the models represent more obscured phases, and should be compared with samples of objects whose near IR colors become very red, and whose optical spectroscopy becomes difficult or impossible with present day instrumentation (e.g. Garcia Lario et al. 1999). In particular, our main test will be made by comparing with the Smith et al. (1995) stars, which are luminous, non obscured AGBs, for which CSE absorption is probably negligible, as it is indicated by their near IR colors.

We compute for our models the flux-weighted optical depth τ_F (e.g. Ivezic & Elitzur 1995), defined as the ratio between the mass loss rate and the classic rate based on the single-scattering approximation, given by the condition that the momentum flow of the gas ($\dot{M}v_{\rm exp}$) equals that of the photons (L/c). The classic value is thus $\dot{M}_{\rm classic} = L/(v_{\rm exp} \cdot c)$, whereas the flux-weighted optical depth τ_F is given by

$$\tau_F = \dot{M} \cdot v_{\rm exp} \cdot c/L$$

Habing et al. (1994) have stressed the possibility of having stars with momentum flow much larger than the gas momentum. To find out the value of τ_F we rely on the results of previous computations, which indicate a dependency of $v_{\rm exp}$ on luminosity of the form $v_{\rm exp} \sim L^{0.25}$ (Jura 1984; Habing et al 1994). In order to have a calibration adequate to the LMC metallicity the constant of proportionality has been fixed by demanding a star with $L = 30000 L_{\odot}$ to have $v_{\rm exp} = 10$ Km s^{-1} (van Loon et al. 1999a). We therefore approximate τ_F by

$$\tau_F = 3.64 \cdot 10^7 \dot{M} (L/L_{\odot})^{-0.75}$$

This is a first order approximation to find out likely values for a physically sound parameter. We have to caution that the LMC expansion velocities are very uncertain (only a few determinations based on noisy data) and the derivation of these velocities also depend on the mass loss rate (Steffen et al. 1998).

We computed τ_F along the evolution of our models. From test computation of the emerging fluxes from the CSE for our models (Groenewegen & Ventura 2000 in preparation), we can make a rough division between models: if $\tau_F \lesssim 0.3$, we can consider the model not much affected by the CSE and include it in the comparison with the lithium data from the Smith et al. (1995) samples, while for $\tau_F \gtrsim 0.3$ the CSE increasingly dominates and the models are to be compared with the samples of obscured stars.

3. Model results

The main aim of this work is to construct a simple population synthesis adequate to describe the Magellanic Clouds upper AGB stars, in order to derive information on the mass loss formulation, which is a physical input very poorly constrained by theory. Consequently, following MDV99 which provides a general description of the new physical inputs adopted in our models and of the detailed results, we now build up models adequate for the chemical composition of the LMC, namely Z=0.01.

The models cover the mass range $3M_{\odot} \leq M \leq 6.5M_{\odot}$ with mass steps of $0.5M_{\odot}$. We built four sets of models corresponding to the values for the parameter η_R in the mass loss formula: η_R = 0.005, 0.01, 0.05 and 0.1. The overshooting parameter was set to $\zeta = 0.02$. In all cases only overshooting from the external border of convective cores is considered; the influence of symmetric overshooting will be discussed in Sect. 6.1. Table 1 lists the computed models and some of the interesting physical quantities. Notice first that the $6.1M_{\odot}$ models ignites carbon at the centre of the star in a semi-degenerate regime, thus jumping the phase of thermal pulses. The table confirms the results obtained by MDV99, and is also consistent with other authors recent main results (Sackmann & Boothroyd 1992; Blöcker et al. 2000; Forestini & Charbonnel 1997), once the differences in the approach to convection, mass loss and the

Table 1. Values of the main physical quantities during the AGB phase for all our models computed.

$\frac{M}{M_\odot}$	$\frac{M^{\rm 1stTP}_{\rm core}}{M_\odot}$	$\log(\frac{L}{L_\odot})^a$	$\frac{M^a_{\rm core}}{M_\odot}$	$T^b_{\rm max}$	$\log(\frac{L}{L_\odot})^b_{\rm max}$	$\Delta t(^7Li)^c$	$\Delta t(^7Li)^d$	$\log(\epsilon(^7Li))_{\rm max}$	${\rm Li-yield}^{\rm e}$
				$\eta_R = 0.005$					
3.0	0.620	4.30	0.779	$6.3 \cdot 10^7$	4.34	$2.0 \cdot 10^5$	$2.0 \cdot 10^5$	3.1	$2.53 \cdot 10^{-9}$
3.3	0.696	4.30	0.782	$6.3 \cdot 10^7$	4.38	$2.0 \cdot 10^5$	$2.0 \cdot 10^5$	3.2	$2.17 \cdot 10^{-9}$
3.5	0.755	4.30	0.794	$6.5 \cdot 10^7$	4.38	$1.7 \cdot 10^5$	$1.7 \cdot 10^5$	3.4	$2.78 \cdot 10^{-9}$
4.0	0.874	4.35	0.881	$7.0 \cdot 10^7$	4.49	$6.5 \cdot 10^4$	$6.5 \cdot 10^4$	3.8	$1.42 \cdot 10^{-10}$
4.5	0.917	4.38	0.918	$7.0 \cdot 10^7$	4.56	$4.5 \cdot 10^4$	$3.9 \cdot 10^4$	3.9	$3.44 \cdot 10^{-10}$
5.0	0.959	4.40	0.959	$7.4 \cdot 10^7$	4.67	$3.3 \cdot 10^4$	$1.7 \cdot 10^4$	4.0	$5.36 \cdot 10^{-10}$
5.5	0.998	4.43	0.997	$7.8 \cdot 10^7$	4.78	$2.3 \cdot 10^4$	$1.0 \cdot 10^4$	4.0	$8.63 \cdot 10^{-10}$
6.0	1.050	4.50	1.030	$8.0 \cdot 10^7$	4.68	$1.4 \cdot 10^4$	$2.0 \cdot 10^3$	4.2	$2.10 \cdot 10^{-9}$
				$\eta_R = 0.01$					
3.3	0.705	4.30	0.782	$6.3 \cdot 10^7$	4.36	$1.9 \cdot 10^5$	$1.9 \cdot 10^5$	3.3	$4.03 \cdot 10^{-10}$
3.5	0.750	4.30	0.793	$6.3 \cdot 10^7$	4.37	$1.7 \cdot 10^5$	$1.7 \cdot 10^5$	3.4	$4.03 \cdot 10^{-10}$
4.0	0.876	4.35	0.878	$7.0 \cdot 10^7$	4.48	$6.3 \cdot 10^4$	$5.5 \cdot 10^4$	3.8	$6.08 \cdot 10^{-10}$
4.5	0.918	4.39	0.918	$7.0 \cdot 10^7$	4.56	$4.4 \cdot 10^4$	$2.6 \cdot 10^4$	3.9	$7.29 \cdot 10^{-10}$
5.0	0.960	4.40	0.960	$7.4 \cdot 10^7$	4.61	$2.8 \cdot 10^4$	$6.7 \cdot 10^3$	4.0	$1.29 \cdot 10^{-9}$
5.5	1.002	4.42	1.001	$7.9 \cdot 10^7$	4.69	$2.2 \cdot 10^4$	$5.7 \cdot 10^3$	4.0	$1.89 \cdot 10^{-9}$
6.0	1.050	4.50	1.050	$8.0 \cdot 10^7$	4.75	$1.4 \cdot 10^4$	$1.0 \cdot 10^3$	4.2	$4.10 \cdot 10^{-9}$
				$\eta_R = 0.05$					
3.3	0.702	-	-	$3.2 \cdot 10^7$	4.27	-	-	0.0	$1.76 \cdot 10^{-11}$
3.5	0.750	4.30	0.795	$6.3 \cdot 10^7$	4.36	$8.0 \cdot 10^4$	$5.7 \cdot 10^4$	3.2	$4.26 \cdot 10^{-10}$
4.0	0.870	4.34	0.876	$7.0 \cdot 10^7$	4.47	$6.2 \cdot 10^4$	$1.5 \cdot 10^4$	3.7	$2.73 \cdot 10^{-9}$
4.5	0.915	4.40	0.916	$7.0 \cdot 10^7$	4.54	$4.0 \cdot 10^4$	$7.0 \cdot 10^3$	3.9	$3.51 \cdot 10^{-9}$
5.0	0.960	4.60	0.960	$7.0 \cdot 10^7$	4.67	$2.7 \cdot 10^4$	$4.0 \cdot 10^3$	4.0	$5.78 \cdot 10^{-9}$
5.5	1.000	4.50	0.996	$7.9 \cdot 10^7$	4.75	$1.9 \cdot 10^4$	$3.0 \cdot 10^3$	4.0	$7.33 \cdot 10^{-9}$
6.0	1.050	4.50	1.052	$8.0 \cdot 10^7$	4.75	$1.3 \cdot 10^4$	$5.0 \cdot 10^2$	4.2	$1.49 \cdot 10^{-8}$
				$\eta_R = 0.1$					
3.5	0.751	-	-	$3.5 \cdot 10^7$	4.28	-	-	0.2	$1.43 \cdot 10^{-11}$
3.7	0.804	4.30	0.820	$6.0 \cdot 10^7$	4.36	$6.0 \cdot 10^4$	-	3.1	$8.08 \cdot 10^{-10}$
4.0	0.875	4.35	0.879	$7.0 \cdot 10^7$	4.46	$5.2 \cdot 10^4$	-	3.8	$4.94 \cdot 10^{-9}$
4.5	0.917	4.39	0.918	$7.0 \cdot 10^7$	4.54	$3.4 \cdot 10^4$	$3.0 \cdot 10^3$	3.9	$6.49 \cdot 10^{-9}$
5.0	0.961	4.43	0.961	$7.0 \cdot 10^7$	4.60	$2.5 \cdot 10^4$	$2.0 \cdot 10^3$	4.1	$9.61 \cdot 10^{-9}$
5.5	1.030	4.44	1.038	$7.9 \cdot 10^7$	4.72	$1.3 \cdot 10^4$	-	4.1	$1.69 \cdot 10^{-8}$
6.0	1.052	4.50	1.050	$7.9 \cdot 10^7$	4.75	$1.0 \cdot 10^4$	-	4.2	$2.31 \cdot 10^{-8}$

[a] Values of luminosities and core masses refer to the beginning of the "super-rich" phase, when $\log(\epsilon(^7Li)) \geq 2$.
[b] These values refer to the time when lithium abundance is at its maximum value.
[c] Total duration (in years) of the phase when $log(\epsilon(^7Li)) \geq 2$.
[d] Total duration (in years) of the phase when $log(\epsilon(^7Li)) \geq 2$ and $\tau_F \leq 0.3$.
[e] The lithium yield is defined as the ratio between the total amount (in mass) of lithium produced within the star and ejected in to the interstellar medium and the initial mass of the star.

different chemistry are taken into account. In the following we describe the feature of models as a function of the mass loss rate, the main input which we are trying to constrain.

3.1. Mass and luminosity at which HBB is achieved

The minimum mass evolving as a Li-rich AGB goes from $3M_\odot$ ($\eta_R = 0.005$) to $3.7M_\odot$ ($\eta_R = 0.1$). A larger mass loss rate in fact triggers an earlier cooling of the outer layers of the star before the ignition of HBB. The minimum core mass required for lithium production ranges from ~ 0.78 to $\sim 0.82M_\odot$, but the corresponding luminosity is always $\log(L/L_\odot) \simeq 4.3$; we therefore expect to find lithium rich sources for $M_{\rm bol} \leq -6$, in excellent agreement with the results of the survey by Smith et al. (1995) and independently from the mass loss rate.

3.2. Lithium yields

Fig. 1 shows the evolution of surface lithium abundance for some models computed with $\eta_R = 0.05$ and 0.01. Note that the $6M_\odot$ model achieves temperatures sufficient to ignite the Cameron-Fowler mechanism well before the beginning of ther-

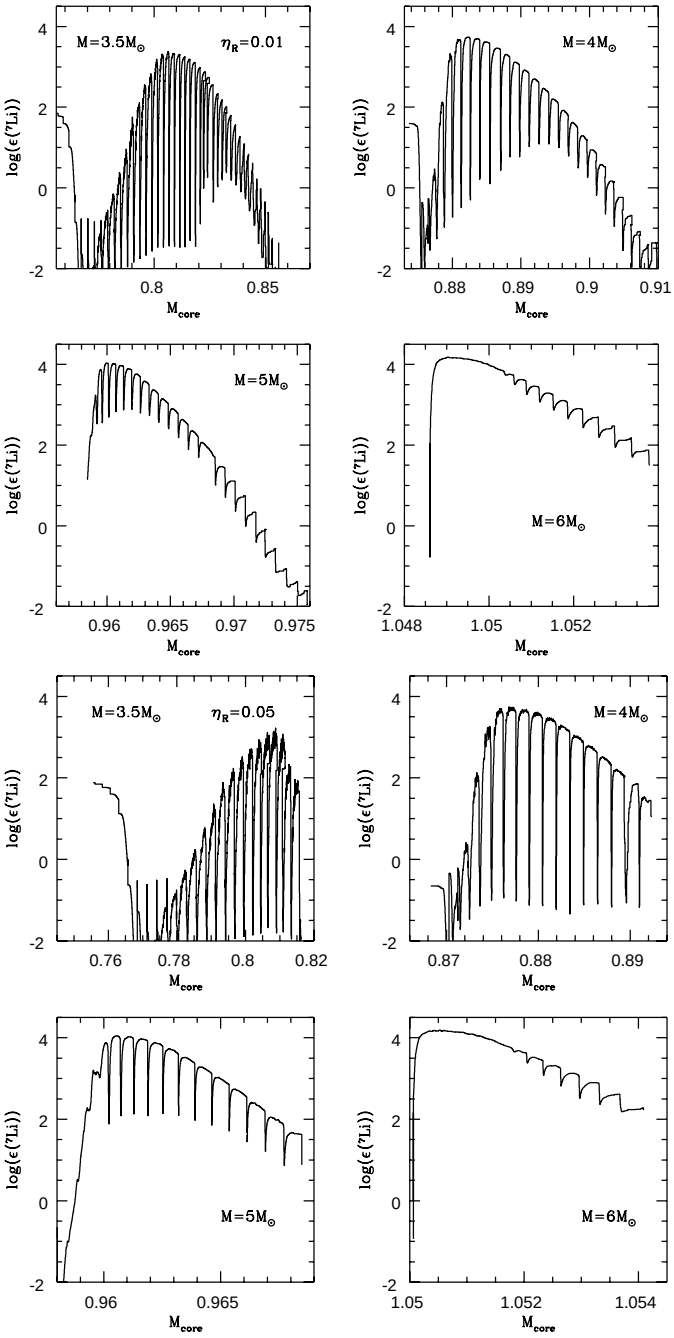

Fig. 1. Evolution in terms of lithium production of some of our intermediate mass models: upper panels refer to computations performed with $\eta_R = 0.01$, lower panels correspond to the case $\eta_R = 0.05$.

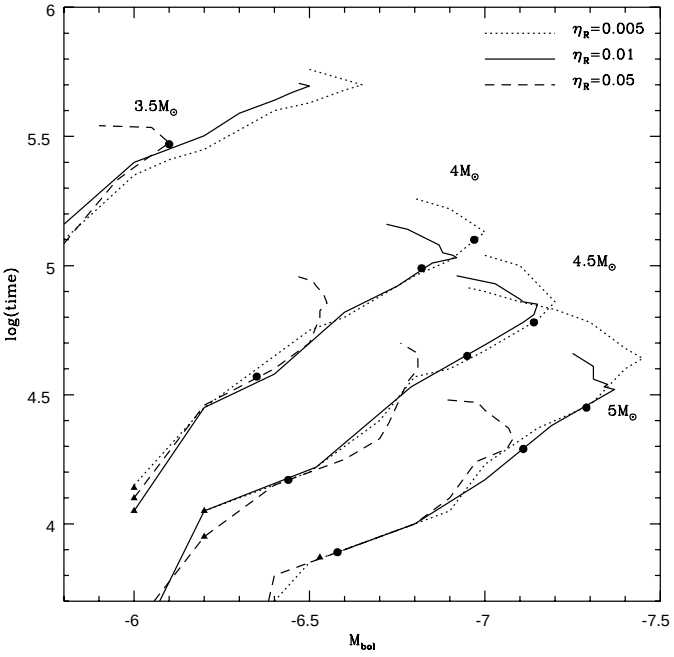

Fig. 2. Evolution of some intermediate mass models computed with $\eta_R = 0.005, 0.01, 0.05$ in the $M_{\rm bol} - \log(age)$ plane. Times were normalized at the beginning of the AGB phase. Triangles along the tracks indicate the location of the first thermal pulse, full circles point the stage at which the optical depth τ_F exceeds 0.3. Note that according to this criterium the $3.5M_\odot$ models computed with the lower values of η_R never become invisible in the optical.

mal pulses, so that when the first pulse starts the lithium abundance is already in the declining branch. A similar behaviour is found in the $M = 5.5M_\odot$ case (not shown).

The largest amount of surface lithium which these stars can produce is a slightly increasing function of initial mass. The phase during which the star shows up lithium rich is obviously shorter for the models of larger η_R, since the larger mass loss rate causes a decline of luminosity and a cooling of the whole external envelope, thus turning off the hot bottom burning.

The last column in Table 1 shows the lithium yield. The masses close to the limit of carbon ignition provide the major contribution, due to the fact that the $5.5, 6M_\odot$ models begin lithium production while the luminosity is still rising, so that the maximum lithium abundance is achieved in conjunction with the largest value of luminosity (and hence of mass loss). For the lowest masses, we note from Table 1 that the yield of the $3.5M_\odot$ models of $\eta_R = 0.005$ are not due to lithium production, but to the survival of lithium from the previous evolutionary phases. As the present abundance of lithium in the ISM is $\log X_{\rm Li} \simeq -8$, starting from the population II abundance of $\simeq -9$, only the models with $\eta_R \gtrsim 0.05$ can significantly contribute to the galactic enrichment of the ISM, should they be consistent with the other evolutionary constraints.

3.3. Mass loss and the duration of the optically bright phase

Fig. 2 shows the time spent in the AGB phase for different masses and $\dot{M}$. The visible phase for each mass ends in correspondence of the full point along the track. The evolution of the flux-weighted optical depth (τ_F) along our sequences with different η_R is shown in Fig. 3. The important evolutionary region is at $-6 \gtrsim M_{\rm bol} \gtrsim -7$ where the bright lithium rich AGBs are located. The mass to be attributed to these stars depends on the mass loss rate: If $\eta_R = 0.01$ or 0.005, the sequences from 3.5 to $4.5M_\odot$ evolve almost completely below $\tau_F = 0.3$, so that these models should never be particularly obscured, and we can

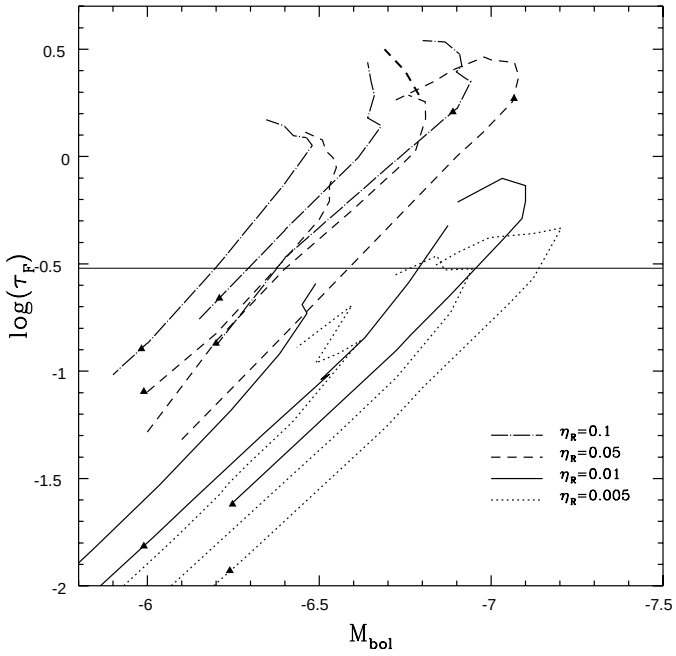

Fig. 3. Evolution of some intermediate mass models computed with $\eta_R = 0.005, 0.01, 0.05, 0.1$ in the $M_{\rm bol} - \log \tau_F$ plane. For $\eta_R = 0.005, 0.01$ we report tracks corresponding to initial masses $M = 3.5, 4, 4.5 M_\odot$, while for $\eta_R = 0.05, 0.1$ we show $M = 4, 4.5, 5 M_\odot$. The heavy-dashed track gives the evolution of a $4.5 M_\odot$ model computed by adopting the Schroeder et al. (1998) mass loss rate from the point when the luminosity was at the top. Continuous horizontal line indicates the threshold value $\tau_F = 0.3$ above which we assume that the star can not be detected in the optical.

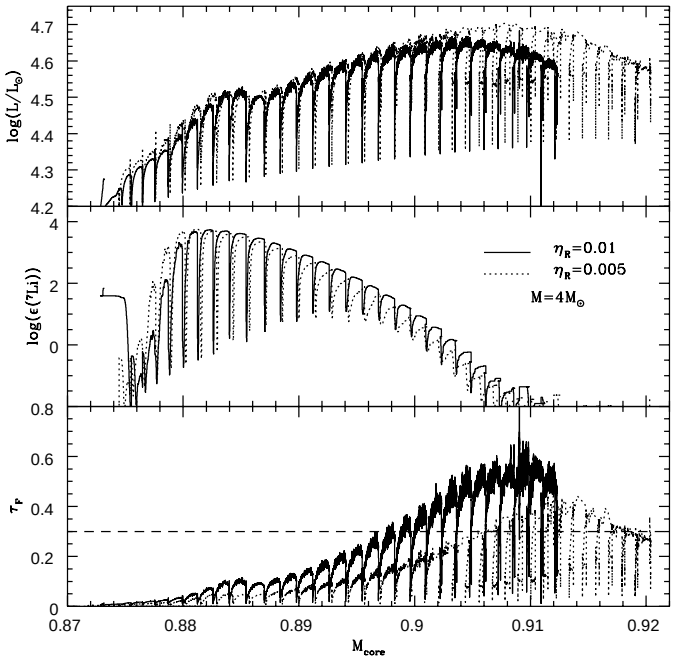

Fig. 4. Comparison between the variations with core mass of some physical and chemical quantities of two $4 M_\odot$ models calculated by assuming two different mass loss rates, corresponding to the Blöcker's recipe with $\eta_R = 0.01$ and $\eta_R = 0.005$. The thin dashed line in the bottom panel indicates the value of τ_F we selected to separate stars still observable in the optical from those heavily obscured. We see that in the $\eta_R = 0.005$ case the optical depth keeps low up to phases when $\log(\epsilon(^7Li))$ has dropped below 0 (middle panel).

expect that these are the masses which populate the AGB. On the contrary, if η_R is as large as 0.05 or 0.1, the sequences below $5 M_\odot$apparently are already obscured when they populate the most luminous bin $-6.5 \gtrsim M_{\rm bol} \gtrsim -7$. For all sequences the evolution proceeds from low τ_F to larger values, at which the CSE dominates. In the end, τ_F may decrease again due to the decrease in the total stellar luminosity and consequent decrease in $\dot{M}$. In the cases $\eta_R = 0.005$ and 0.01 the models evolve considerably in luminosity at low τ_F, that is when they have no appreciable CSE, while for the larger η_R cases the part of the sequence not affected by the CSE is only a small fraction. In other words, the larger is $\dot{M}$, the shorter is the TP phase during which the model represents a luminous AGB star corresponding to the Smith et al. (1995) sample. In particular, the $6 M_\odot$ sequence of $\eta_R = 0.05$ and 0.1 would evolve into a dust embedded phase even *before* they start the thermal pulse phase. Can we find a way of discriminating, at least qualitatively, between the four rates? We will try to do this using the luminosity and number distribution of lithium rich AGBs.

3.4. Mass loss and Lithium evolution

Fig. 4 shows the effect of mass loss on the luminosity evolution of two $4 M_\odot$ models computed with $\eta_R = 0.01, 0.005$. The variation with core mass of luminosity, lithium and optical depth τ_F are reported. We see that the evolution in luminosity is slightly different: in the $\eta_R = 0.01$ case $\log(L/L_\odot)$ attains a maximum value of 4.67 when the core mass is $M_{\rm core} \sim .904 M_\odot$. In the $\eta_R = 0.005$ model the luminosity attains its maximum of $\log(L/L_\odot) = 4.71$ when $M_{\rm core} = 0.908 M_\odot$. At this point the difference between the bolometric magnitudes of the two models is 0.13 mag.

The bottom panel shows that for a fixed value of the core mass (hence, of luminosity) the optical depth in the $\eta_R = 0.005$ case is approximately half the value of the $\eta_R = 0.01$ case, making the star visible for a longer time. The main difference between the two models is therefore that *in the $\eta_R = 0.005$ case the star remains visible in the optical until phases when the lithium abundance has already dropped to low values, due both to the very large $T_{\rm bce}$'s and to the exhaustion of ^3He in the external envelope*. Observationally we would expect in the latter case to detect several large luminosity sources with negligible amounts of lithium.

4. Numeric simulations of the optically bright AGB phase

To have more quantitative informations, we compute simple population synthesis for a sample of stars which go through the HBB phase described. We assume an IMF with exponent -2.3 for the mass distribution and consider that the range of evolving masses is limited in between 3.0 and $6 M_\odot$. The evolutionary

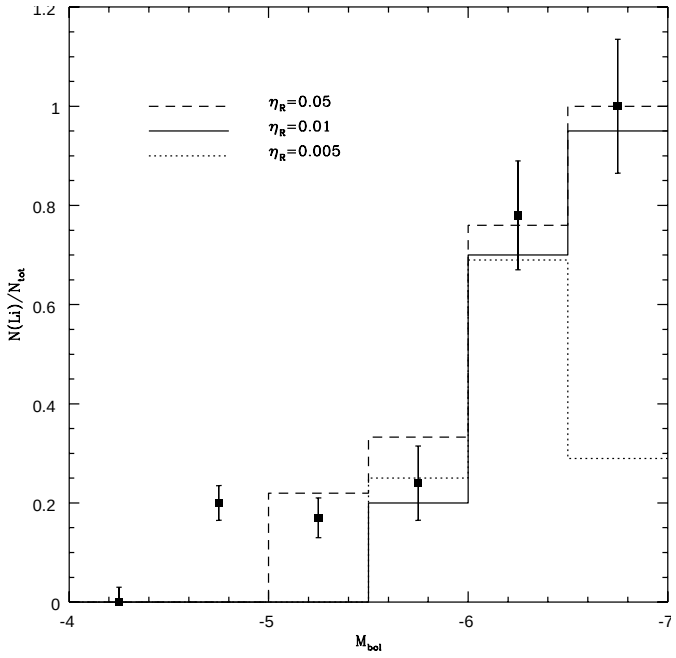

Fig. 5. Frequecy histogram of lithium rich AGBs as a function of $M_{\rm bol}$, for three sets of models with different mass loss rates. Dots indicate the frequencies related to the survey of the most luminous AGBs in the MCs by Smith et al. (1995). In the smallest $\dot{M}$ case ($\eta_R = 0.005$) we would expect the majority of AGB sources with $-7 \leq M_{\rm bol} \leq -6.5$ to have negligible surface lithium, leading to a strong discrepancy with the observational evidence.

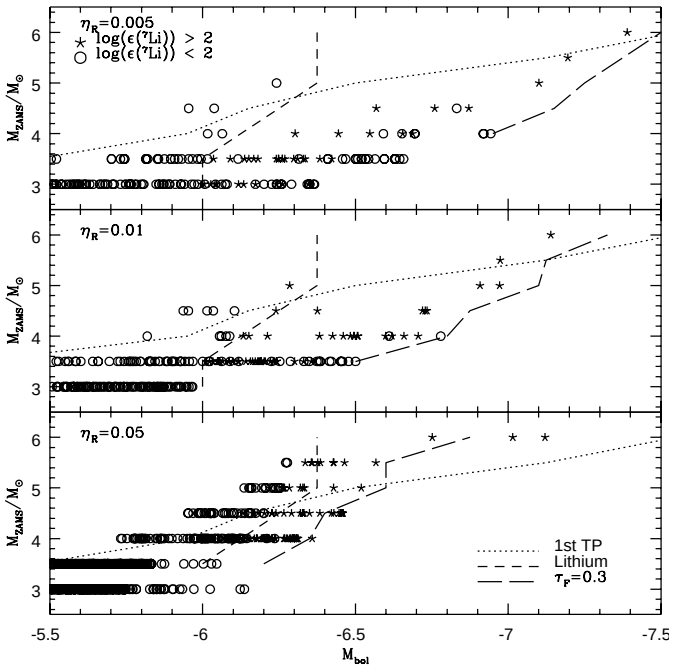

Fig. 6. Numerical simulations for the distribution of our AGB models in the magnitude - mass plane, obtained by assuming that the sources become invisible in the optical as soon as τ_F becomes equal to 0.3. Results for $\eta_R = 0.005, 0.01, 0.05$ are reported. Also shown are the lines indicating the first thermal pulse for each mass (dotted), the points where Li-rich abundances are achieved (dashed), and the limit of detectability in the optical (long-dashed). The relatively low number of stars with masses $M > 4M_\odot$ is due to the difference among the various models in terms of AGB life times; for the sake of clarity a flat mass function has been adopted in building this figure.

tracks are considered only until the models have $\tau_F \lesssim 0.3$. We extract randomly the value of the initial mass and then allocate it at an age (an thus a luminosity) chosen randomly again in the time interval between the beginning of the AGB phase and the $\tau_F = 0.3$ time (this is equivalent to assume a constant birthrate between now and the time at which the lowest masses considered - $3M_\odot$ - evolve, i.e. $4 \cdot 10^8$ yr).

We show in Fig. 5 the result of our simulations for the ratio of lithium rich AGBs versus their total number in intervals of 0.5 mag in $M_{\rm bol}$, compared with the Smith at al. (1995) data (from their Fig. 9). The comparison must be limited to the bins of $-6 \gtrsim M_{\rm bol} \gtrsim -7$, which correspond to the models which manifacture lithium (in fact the bins at $M_{\rm bol} \geq -6$ in our models correspond to the early AGB phases, during which the temperature at the base of the envelope was not large enough to destroy the surface lithium remnant of the previous evolution, while the stars at $M_{\rm bol} \geq -6$ in Smith et al. (1995) show strong evidences of s-processes enrichment, and are thus likely a result of AGB evolution of sources with initial masses below $M_{ZAMS} \sim 3M_\odot$, which are not considered here, so the good agreement with our models at these magnitudes is fortuitous).

The main result of Fig. 5 is that the lowest mass loss rate ($\eta_R = 0.005$) predicts that only about 20% of AGBs in the bin -6.5 $\gtrsim M_{\rm bol} \gtrsim -7$ should be lithium rich, while in the Smith et al. sample almost all these stars are lithium rich. (In fact there are two SMC stars without lithium at $M_{\rm bol} \sim -7$. This is included in the poissonian error bar of our Fig. 5).

The result can be understood by looking at Fig. 6, where we report the outcome of our simulations made for the three mass loss rates adopted considering a flat mass function and taking into account all masses $3M_\odot \leq M_{ZAMS} \leq 6M_\odot$. The flat IMF has no incidence upon our main findings in terms of the fraction of Li-rich stars found in the various bins of magnitude, and has the advantage of showing up more clearly the results.

In Fig. 6 we also show the line at which TPs begin (dotted), where the stars become Li-rich (dashed line), and where τ_F reaches the value of 0.3 (long dashed). We consider first the $\eta_R = 0.005$ case (top panel of Fig. 6). Here the $3.5M_\odot$ model reaches luminosities $M_{\rm bol} \leq -6.5$ before strong mass loss leads to a decline in the luminosity. In these final stages of the evolution the surface lithium is exhausted because of the lack of ^3He within the envelope, so that, considering the longer life-times of the $3.5M_\odot$ model, we expect that the majority of stars at $-7 \leq M_{\rm bol} \leq -6.5$ have no lithium, as in fact shown in Fig. 5. The mass loss rate corresponding to such η_R seems therefore to be too low.

In the $\eta_R = 0.01$ case (middle panel of Fig. 6) the rise of luminosity in the $3.5M_\odot$ model is halted by the mass loss in the final stages of the evolution, therefore stars with magnitudes $-7 \leq M_{\rm bol} \leq -6.5$ are the descendants of masses $M \geq 4M_\odot$. Note that, within this framework, stars with initial masses $M \geq$

$5.5M_\odot$ populate this region before the beginning of TPs: these latter sources, however, would constitute less than 5% of the whole population.

In the $\eta_R = 0.05$ case, mass loss is so large that only masses $M \geq 5M_\odot$ can ever reach stages where $M_{\rm bol} \leq -6.5$. But these stars would cross this interval of magnitudes well before the first TP, as can be seen following the dotted line in Fig. 6. Although modelling of the third dredge-up is still uncertain, it is qualitatively necessary that the stars suffer TPs to have the possibility to dredge-up s-process elements, as already discussed in Sect. 2. Therefore the stars corresponding to $M \sim 5.5 - 6M_\odot$ would not display any evidence of s-process elements enrichment; this is in contrast with the observations of AGBs in the MCs, which show enrichment of s-process elements in all the Li-rich sources. On the basis of this discussion we may conclude that $\eta_R < 0.05$ is required.

The case $\eta_R = 0.01$ seems to provide the best agreement between our models and the observations of AGBs in the MCs. This would indicate that the most luminous Li-rich AGBs in the MCs are the descendants of stars with initial masses $M \sim 4 - 4.5M_\odot$. In MDV99 we had identified these most luminous stars with the evolution of the $6M_\odot$ models: this was due to our neglect of the "visible" phase, and also to the neglect of the information deriving from s-process enhancement in the MC stars.

One uncertain point in the above discussion is the threshold value of $\tau_F^{\rm max} = 0.3$ at which we assume that the stars become invisible in the optical. We tested the sensitivity of our main conclusions to the choice of such $\tau_F^{\rm max}$. A variation by 0.1 in $\tau_F^{\rm max}$ shifts the long dashed line in Fig. 6 horizontally by about 0.15 mag. The case $\eta_R = 0.005$ case can be ruled out anyway, since the evolution of the $3.5M_\odot$, which is the main contributor to the population at $-7 \leq M_{\rm bol} \leq -6.5$, has $\tau_F < 0.1$. Therefore even lowering $\tau_F^{\rm max}$ by 50% we still would expect the majority of the most luminous AGBs to be without lithium. In the $\eta_R = 0.05$ case the major difficulty is to populate the region $-7 \leq M_{\rm bol} \leq -6.5$ for stars with masses $M < 5M_\odot$: this problem still holds by varying $\tau_F^{\rm max}$, because $\dot{M}$ attains so large values that masses $M \sim 4 - 4.5M_\odot$ cannot reach such luminosities anyway. The evolution of the more massive models is in contrast with the presence of s-enrichment; in order to have their evolution observable well after the beginning of the TP phase, $\tau_F^{\rm max}$ should be ≥ 0.6, value really very large to be compatible with the "normal" colors of the Smith et al. (1995) sample. What can be said for $\eta_R = 0.01$? In this case the agreement with the observations is due to the fact that the evolution of the $3.5M_\odot$ model never reaches luminosities as large as $M_{\rm bol} \sim -6.5$. The last bin in Fig. 5 would be mainly populated by stars with $M_{ZAMS} \sim 4 - 4.5M_\odot$, in a phase when they are Li-rich. By adopting a smaller $\tau_F^{\rm max}$ we expect on the average a lower abundance of s-process elements, but the percentage of Li-rich luminous AGBs would be close to 100%. Our numerical simulations show that the results are almost completely unchanged if we adopt a larger $\tau_F^{\rm max}$, because in this latter case the same sources would be observable up to later stages when their luminosity exceeds $M_{\rm bol} \sim -7$, thus populating a region

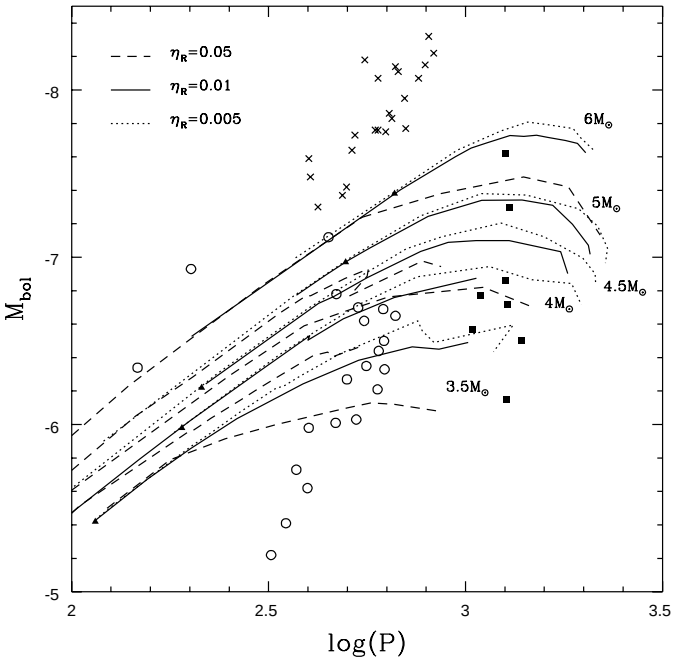

Fig. 7. Evolution of some $\eta_R = 0.005, 0.01, 0.05$ models in the $\log(P) - M_{\rm bol}$ plane (right), where P is the period expressed in days. Full triangles along the tracks indicate the first thermal pulse; open points and crosses refer to the AGB (points) and supergiant (crosses) stars in the LMC sample given by Wood et al. (1983); full squares correspond to the sample of obscured AGB stars in the LMC found in Wood et al. (1992).

out of the limits $-7 \leq M_{\rm bol} \leq -6.5$. No such luminous AGBs have been observed in the quoted survey, so that a value of $\tau_F^{\rm max}$ largely exceeding 0.3 is probably to be excluded.

If our calibration of η_R is valid, from Table 1 we easily recognize that these AGBs can not influence in any appreciable way the galactic increase of the lithium abundance from its population II value ($\log(\epsilon(^7Li)) \sim 2.2$) to the popI standard value of $\log(\epsilon(^7Li)) \sim 3.1$. Full consideration of this problem will be given in a following work (Ventura & Romano, in preparation).

5. The obscured phase

5.1. Pulsation period evolution

The computations so far performed allow us further comparisons with other sets of data. The evolution of our models in the $\log(P) - M_{\rm bol}$ plane is shown in Fig. 7 together with the samples by Wood et al. (1983) and Wood et al. (1992). Fig. 7 shows that the evolutionary sequences first cover the luminous long period variables region (Wood et al. 1983, open circles) and then evolve to longer periods, where they match the location of OH/IR stars in the Wood et al. (1992) sample, at periods above 1000d (filled squares). The sequences with initial masses $4M_\odot \leq M \leq 4.5M_\odot$ traverse the region $-7 \leq M_{\rm bol} \leq -6.5$, which correspond to the last bin in Fig. 5. For $\eta_R = 0.01$ their τ_F does not exceed 0.3 (see Fig. 3), and so we can expect that the models describe stars which are not particularly obscured. The most massive AGB sequences ($M_{ZAMS} = 6M_\odot$) with

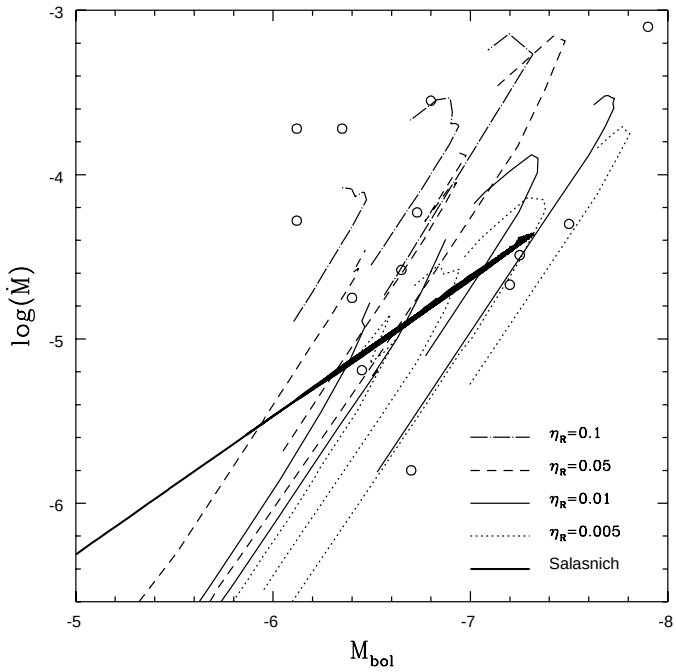

Fig. 8. Variation with luminosity of the mass loss rate (expressed in $M_{\odot}/$yr units) of some models computed with different prescriptions for $\dot{M}$. In the $\eta_R = 0.005, 0.01$ cases we show the evolution of masses $3.5M_{\odot} \leq M \leq 5M_{\odot}$, for $\eta_R = 0.05, 0.1$ we report tracks for $M = 4, 5, 6M_{\odot}$. The heavy line corresponds to a $5M_{\odot}$ model computed by adopting the Salasnich et al. (1999) formula. Open points indicate the results concerning LMC sources given in van Loon et al. (1999a).

low η_R reach luminosities as large as $M_{\rm bol}\sim -7.5$, at periods exceeding 1000 days, and could represent the two large luminosity, very long period stars shown. In fact, the evolution of the $6M_{\odot}$ models not only reaches such a luminous $M_{\rm bol}$, but has a large τ_F, pointing to stars with strong CSE. Certainly, we predict that these two stars are lithium rich, but they are probably not observable in the red part of the visible spectrum.

5.2. Other mass loss formulations

Fig. 3 shows that the somewhat simple minded parameter τ_F is not costantly increasing during the evolution. It may well be that in some cases the decrease of the stellar luminosity leads to such a reduction of $\dot{M}$ that the objects becomes less obscured. Stop of HBB can in that case also lead to the late formation of a carbon star (Frost et al. 1998). The reduction in τ_F depends on the mass loss formulation we have adopted. We shortly show comparison with other formulations. The evolution of a $4.5M_{\odot}$ model has also been computed by applying a correction of the form ${T_{\rm eff}}^{-8}$ to Blöcker's recipe with $\eta_R = 0.05$ (heavy-dashed line in Fig. 3): the net result is that the effect of the decline of luminosity is completely counterbalanced by the decrease of $T_{\rm eff}$, so that the optical depth of the star is still large. Thus the large mass loss rates obtained with $\eta_R = 0.1$ can be also obtained with a strong dependence on $T_{\rm eff}$.

We finally tested the Salasnich et al. (1999) recipe for mass loss. Fig. 8 shows the variation with luminosity of various models computed with η_R in the range $0.005-0.1$ and a $5M_{\odot}$ model computed with the Salasnich et al. (1999) recipe. We can clearly distinguish the different slope of the latter prescription with respect to the others. The corresponding $\dot{M}$, particularly at large luminosities, turns out to be too low: a $3.5M_{\odot}$ evolution would last in the non-obscured phase for $\sim 10^5$ yr at $M_{\rm bol} \sim -6.5$ after all lithium has been already burned (like in the $\eta_R = 0.005$ case), in contrast with the observations.

5.3. Comparison with other mass loss informations

Fig. 8 shows values of $\dot{M}$ by detailed computations by van Loon et al. (1999a), based on IR observations of several sources in the LMC (Schwering & Israel 1990; Reid et al. 1990): we should remember of course that the observed $\dot{M}$'s have several uncertainties connected with the assumptions made concerning the expansion velocities and the dust to gas ratio, and are time averaged due to the IR photometry. A precise fit cannot be expected. Also, $M_{\rm bol}$ should be treated with some care since the distance to the LMC is subject to discussion (published range covers 0.4 mag at present) and $M_{\rm bol}$ is itself uncertain by $0.1 - 0.2$ mag for variable, red stars.

Values of $\eta_R = 0.1$ seem to be a very upper limit: our $6M_{\odot}$ model computed with such η_R attains values of $\dot{M}$ which in some cases exceed the largest observed values. The large spread of the points in Fig. 8 shows the difficulty of fitting the observational evidence with a single mass loss rate, suggesting a possible spread of values of η_R.

It is important here to remember that these values for η_R apply to the relationships $M_{\rm core} - M_{ZAMS}$ and $M_{\rm core}$ - luminosity provided by *our own models*. Our models provide the largest core masses in the literature (Wagenhuber & Groenewegen 1998), and use of the FST model of turbulent convection leads to a steeper core mass - luminosity relationship with respect to MLT models (D'Antona & Mazzitelli 1996): due to the steep dependence of Blöcker's recipe on luminosity, both these effects lead to larger mass loss rates in our models during the AGB phase. MLT models would require larger values of η_R. The conclusions on the lithium yields, however, would remain valid.

6. Overshooting

6.1. Symmetric overshooting

Models computed in the present work do not include any extramixing from the base of the external envelope. Here we focus our attention on how "overshooting from below" might change our results. The larger extension of the inward penetration of the convective envelope following each pulse, in the symmetric overshooting models, brings some helium at the surface of the star, thus delaying the ignition of the following pulse. The interpulse phase is ~ 3 times longer. The delay in the occurrence of thermal pulse causes the pulse to be ignited at larger temperatures, so that its strength is enhanced.

Fig. 9 shows the variation with time of the surface abundances of carbon and lithium during the AGB phase for both

Table 2. Values of some physical quantities of the evolution of $4M_{\odot}$ models computed with different values of the overshooting parameter ζ.

$\frac{\zeta}{H_p}$	$\frac{M_{\rm core}^{\rm 1stTP}}{M_{\odot}}$	$\log(\frac{L}{L_{\odot}})^a$	$\frac{M_{\rm core}^a}{M_{\odot}}$	$\log(\frac{L}{L_{\odot}})_{\rm max}$	$\frac{M_{\rm core}^b}{M_{\odot}}$
0.00	0.775	4.30	0.802	4.40	0.835
0.02	0.870	4.34	0.870	4.45	0.890
0.03	0.880	4.34	0.885	4.45	0.900

[a] Values of luminosities and core masses at the beginning of the phase when $\log(\epsilon(^7Li)) \geq 2$.
[b] Values at which $\log(\epsilon(^7Li))$ declines again below 2.

the standard and the symmetric overshooting model of initial mass $M = 4M_{\odot}$. Overshooting from below can no longer be neglected if we are interested in the surface abundance of elements like ^{12}C, which are carried to the stellar surface from internal layers during the third dredge-up: in particular the "carbon star" phase cannot be achieved by the standard model. Although it is not yet monitored in our models, the third dredge-up will also be necessary to bring at the surface the s-process elements manifactured inside the star by the $^{13}C + \alpha$ neutron source (a ^{13}C pocket is naturally created by our overshooting treatment, see MDV99). The lithium rich AGBs in the MCs are s-process enhanced, although the enhancement decreases with the luminosity, as would be expected if higher masses, suffering a smaller number of thermal pulses and a smaller number of dredge-up episodes, populate the high luminosity regions. The third dredge-up is very much model dependent, and no agreement yet has been reached among researchers on its modalities (Lattanzio 1986; Straniero et al. 1997; Herwig et al. 1997), mainly because overshooting cannot be modelled by first principles. On the contrary, the bottom panel of Fig. 9 shows that the evolution of the surface lithium abundance is unchanged in models including overshooting, so that lithium production and its correlation with luminosity, which we have used to calibrate the mass loss, can be regarded as a robust result, independent of the inclusion or not of overshooting from below.

6.2. The influence of ζ

The results given in the previous section, particularly for that concerning the interval of initial masses which are involved in lithium production, are dependent at a certain extent on the amount of overshooting assumed from the Schwarzschild border of convective cores during phases of central burning, i.e. on the value of the parameter ζ. The way the results change with ζ is straightforward: a larger overshooting distance leads to larger core masses at the beginning of TPs, and, for a given initial mass, the probabilities of ignition of the Cameron-Fowler mechanism increases. Consequently, a larger ζ would shift downwards the interval of masses given in the previous section.

To quantify the sensitivity of the results obtained on the value of ζ assumed for the present computations we compare in Table 2 the results of three $4M_{\odot}$ evolutions computed, respectively, with $\zeta = 0, 0.02$ and 0.03. We see that there is a

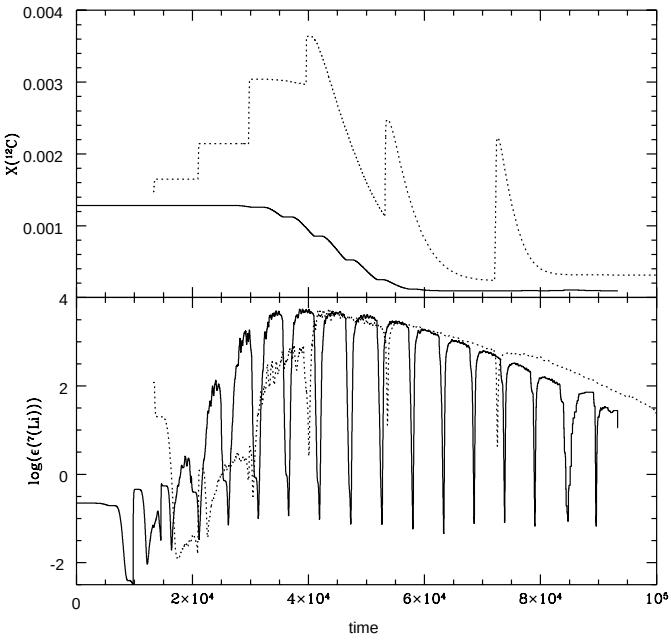

Fig. 9. Evolution of surface chemical abundances of carbon and lithium for the $4M_{\odot}$ models computed by assuming just overshooting from the convectice core of the star during the phases of central nuclear burning (solid track), or also symmetric overshooting from the base of the external convective envelope (dotted).

difference of about $\sim 0.1M_{\odot}$ between core masses at the first TP of the $\zeta = 0$ and $\zeta = 0.02$ cases, while the difference between the two overshooting models corresponding to $\zeta = 0.02$ and $\zeta = 0.03$ is $\sim 0.01M_{\odot}$. This result indicates that a variation of 50% of the overshooting parameter leads to differences in terms of core masses which are well below those triggered by a $0.5M_{\odot}$ shift in the total mass of the star, as seen in Table 1. This is also confirmed by the evolution of the $4M_{\odot}$ model without overshooting, which achieves lithium production and by a $3M_{\odot}$ model with $\zeta = 0.03$, which fails to do so. We also computed an extensive grid of models in the range $5.5M_{\odot} \leq M \leq 6.5M_{\odot}$. By adopting $\zeta = 0.02$ we found that the maximum value of M wich does not ignite ^{12}C in a semi degenerate regime is $M = 6M_{\odot}$, while for $\zeta = 0.03$ this limit is $M = 5.8M_{\odot}$. On the basis of these results we can conclude that the range of $3.5M_{\odot} \leq M \leq 6M_{\odot}$ derived in the previous section is well extablished within $\sim 0.5M_{\odot}$.

7. Conclusions

In this paper we have presented grids of intermediate mass models of metallicity appropriate for the LMC AGBs, Z=0.01, in order to reproduce the observed trend lithium vs luminosity, found by the survey of both Magellanic Clouds by Smith et al. (1995). We found that the interval of initial masses involved in lithium production is well defined within $0.5M_{\odot}$ even considering all the uncertainties connected with the overshooting distance and the mass loss rate, and it is $3.5M_{\odot} \leq M \leq 6M_{\odot}$. More particularly, models with initial masses $M \geq 5.5M_{\odot}$ display a very

peculiar behaviour, since they produce lithium even before the beginning of the first pulse.

Numerical simulations lead to the conclusion that large mass loss rates, approaching $10^{-4}M_{\odot}$ yr^{-1}, are required to fit the observations, otherwise we would expect to detect several large luminosity sources ($M_{\rm bol} \lesssim -6.5$) with negligible amount of lithium in their envelope, while the afore mentioned survey shows that practically all the AGB sources in the MCs with $M_{\rm bol} \leq -6.5$ are lithium rich; if we rely on Blöcker's recipe for mass loss, we find that a value of the free parameter of $\eta_R = 0.01$ is required in our models, while values $\eta_R \geq 0.05$ can be disregarded since in these cases the most luminous Li-rich AGBs would have progenitors masses $M_{ZAMS} \gtrsim 5.5M_{\odot}$. These latter would produce lithium before they have TPs, so that they would not have s-process enriched envelopes, in contrast with the Smith et al. (1995) results.

We conclude that the most luminous Li-rich AGBs in the LMC represent the early AGB phases of the evolution of stars with initial masses $M \sim 4 - 4.5M_{\odot}$. Our models of large progenitor mass ($M \sim 6M_{\odot}$) seem to be able to give a theoretical explanation of the existence in the LMC of AGB sources at $M_{\rm bol} = -7.3$ and -7.6, which are long period, obscured variables (Wood et al 1992).

As a consequence of our calibration of mass loss, massive AGBs should not contribute significantly to the Lithium enrichment of the interstellar medium.

Acknowledgements. P.Ventura thanks M.Groenewegen for helpful discussions. We also thank B.Plez for useful informations on Li-rich AGBs and the referee A.Zijlstra for a very useful report.

References

Abia C., Boffin H.M.J., Isern J., Rebolo R., 1991, A&A 245, L1
Alongi M., Bertelli G., Bressan A., Chiosi C., 1991, A&A 244, 95
Blanco V.M., McCarthy M.F., Blanco B.M., 1980, ApJ 242, 938
Blöcker T., 1995, A&A 297, 727
Blöcker T., Herwig, F., Driebe T., 2000, In: D'Antona F., Gallino R. (eds.) The Changes in Abundances in Asymptotic Giant Branch Stars. Mem. Soc. Astron. Ital., in press
Bonifacio P., Molaro P. 1997, MNRAS 285, 847
Bowen G.H., 1988, ApJ 329, 299
Cameron A.G., Fowler W.A., 1971, ApJ 164, 111
Canuto V.M., Goldman I., Mazzitelli I., 1996, ApJ 473, 550
Canuto V.M., Mazzitelli I., 1991, ApJ 370, 295
Canuto V.M., Mazzitelli I., 1992, ApJ 389, 724
Costa E., Frogel J.A., 1996, AJ 112, 2607
D'Antona F., Mazzitelli I., 1996, ApJ 470, 1093
Feast M.W., 1991, In: de Jager C., Nieuwenhuijzen H. (eds.) Instabilities in Evolved Super and Hyper-Giants
Forestini M., Charbonnel C., 1997, A&AS 123, 241
Frogel J.A., Persson S.E., Cohen J.G., 1980, ApJ 240, 785
Freytag B., Ludwig H.G., Steffen M., 1996, A&A 313, 497
Frost C.A., Cannon R.C., Lattanzio J.C., Wood P.R., Forestini M., 1998, ApJ 332, L17
Garcia Lario P., D'Antona F., Lub J., Plez B., Habing H.J., 1999, In: IAU Symp. 191, Asympotic Giant Branch Stars. ASP, p. 91
Grossman S.A., 1996, MNRAS 279, 305
Habing H.J., 1996, A&AR 7, 97
Habing H.J., Tignon J., Tielens A.G.G.M., 1994, A&A 286, 523
Herwig F., Blöcker T., Schönberner D., El Eid M., 1997, A&A 324, L81
Iben I. Jr., 1975, ApJ 196, 525
Iben I. Jr., 1981, ApJ 246, 278
Iben I. Jr., Renzini A., 1983, ARA&A 21, 271
Ivezic Z., Elitzur M., 1995, ApJ 445, 415
Jura M., 1984, ApJ 282, 200
Lattanzio J.C., 1986, ApJ 311, 708
Lesieur M., 1987, Turbulence in Fluids. Nijhoff, Dordrecht
Maeder A., Meynet G., 1989, A&A 210, 155
Mazzitelli I., D'Antona F., Ventura P., 1999, A&A 348, 846
Meynet G., Mermilliod J.C., Maeder A., 1993, A&AS 98, 477
Mould J.R., Reid N., 1987, ApJ 321, 156
Plez B., Smith V.V., Lambert D.L., 1993, ApJ 418, 812
Reid N., Tinney C., Mould J., 1990, ApJ 348, 98
Romano D., Matteucci F., Molaro P., Bonifacio P., 1999, A&A 352, 117
Sackmann I.J., Boothroyd A.I., 1992, ApJ 392, L71
Sackmann I.J., Smith R.L., Despain K.H., 1974, ApJ 187, 555
Salasnich B., Bressan A., Chiosi C., 1999, A&A 342, 131
Schroeder K.P., Winters J.M, Arndt T.U., Seldmayr E., 1998, A&A 335, L9
Schwarzschild M., Harm R., 1965, ApJ 142, 855
Schwarzschild M., Harm R., 1967, ApJ 145, 496
Schwering P.B.W., Israel F.P., 1990, A catalog of IRAS sources in the Magellanic Clouds. Kluwer, Dordrecht
Smith V.V., Lambert D.L., 1989, ApJ 345, L75
Smith V.V., Lambert D.L., 1990, ApJ 361, L69
Smith V.V., Plez B., Lambert D.L., 1995, ApJ 441, 735
Spite F., Spite M., 1993, A&A 279, L9
Steffen M., Szczerba R., Schönberner D., 1998, A&A 337, 147
Stothers R.B., Chin C.W., 1991, ApJ 381, L67
Straniero O., Chieffi A., Limongi M., et al., 1997, ApJ 478, 332
van Loon J.T., Zijlstra A.A., Whitelock P.A., et al. 1997, A&A 325, 585
van Loon J.T., Groenewegen M.A.T., de Koter A., et al., 1999a, A&A 351, 559
van Loon J.T., Zijlstra A., Groenewegen M.A.T., 1999b, A&A 346, 805
Vassiliadis E., Wood P.R., 1993, ApJ 413, 641
Ventura P., D'Antona F., Mazzitelli I., 1999, ApJ 524, L111
Ventura P., Zeppieri A., Mazzitelli I., D'Antona F., 1998, A&A 334, 953
Wagenhuber J., Groenewegen M.A.T., 1998, A&A 340, 183
Weigert A., 1966, Z. für. Astroph. 64, 395
Willson L.A., Bowen G.H., Struck C., 1996, In: Leitherer C., et al. (eds.) From Stars to Galaxies. ASP Conf. Series 98, 197
Wood P.R., Bessel M.S., Fox M.W., 1983, ApJ 272, 99
Wood P.R., Whiteoak J.B., Hughes S.M.G., et al., 1992, ApJ 397, 552
Xiong D.R., 1985, A&A 150, 133
Zijlstra A.A., Loup C., Waters L.B.F.M., et al., 1996, MNRAS 279, 32